HHS Public Access

Author manuscript

Ann N Y Acad Sci. Author manuscript; available in PMC 2019 February 01.

Published in final edited form as:

Ann N Y Acad Sci. 2018 February ; 1413(1): 25–34. doi:10.1111/nyas.13539.

The unfolding landscape of the congenital myasthenic syndromes

Andrew G. Engel, **Xin-Ming Shen**, and **Duygu Selcen**

Department of Neurology, Mayo Clinic, Rochester, Minnesota

Abstract

Congenital myasthenic syndromes (CMS) are heterogeneous disorders in which the safety margin of neuromuscular transmission is impaired by one or more specific mechanisms. Since the advent of next-generation sequencing methods, the discovery of novel CMS targets and phenotypes has proceeded at an accelerated rate. Here, we review the current classification of CMS and describe our findings in five of these targets identified and investigated in our laboratory in the past 5 years. Defects in LRP4 hinder synaptic development and maintenance; the defects in PREPL are predicted to diminish filling of the synaptic vesicle with acetylcholine; and defects in SNAP25, Munc13-1, and synaptotbrevin-1 impede synaptic vesicle exocytosis.

Keywords

congenital myasthenic syndromes; LRP4; PREPL; SNAP25B; Munc13-1; synaptobrevin

Introduction

During the past 5 years, an increasing number of patients suffering from congenital myasthenic syndromes (CMS) and several novel CMS were identified by different investigators. Figure 1 indicates the currently recognized CMS, and Table 1 shows a classification of 358 CMS kinships investigated at the Mayo Clinic to date. The CMS are grouped according to the (1) anatomic location of the disease protein, (2) defects in glycosylation of proteins required for neuromuscular transmission, (3) defects in the development and maintenance of the neuromuscular junction, and (4) miscellaneous other syndromes that compromise the safety margin of neuromuscular transmission. Below, we focus on recently identified CMS investigated in our laboratory in the past 5 years.

LRP4-related protein 4 (LRP4) myasthenia[1, 2]

LRP4 (LRP4 low-density lipoprotein receptor-related protein 4) is a component of the pathway essential for endplate (EP) development and maintenance. In this pathway, agrin secreted by the nerve terminal into the synaptic space binds to LRP4 attached to the postsynaptic membrane. The agrin–LRP4 complex binds to and activates the receptor

Address for correspondence: Andrew G. Engel, MD, Mayo Clinic, 200 First St., Rochester MN, 55905. age@mayo.edu.

Competing interests

The authors declare no competing interests.

tyrosine kinase muscle-specific kinase (MuSK). This enhances MuSK phosphorylation and leads to clustering of LRP4 and MuSK on the postsynaptic membrane. Activated MuSK, in concert with postsynaptic DOK-7 and other postsynaptic proteins, acts on rapsyn to concentrate the acetylcholine receptor (AChR) in the postsynaptic membrane, enhances synapse-specific gene expression, and promotes postsynaptic differentiation. The same signaling pathway is also essential for maintaining the structure of the adult neuromuscular junction.[3] We identified mutations in *LRP4* in a sporadic patient[1] and in two sisters.[4]

The sporadic patient harbored two heteroallelic mutations in *LRP4*, p.Glu1233Lys c. 3679G>A) and p.Arg1277His (c.3830G>A). At age 17 years, she had moderately severe fatigable weakness and a significant electromyography (EMG) decrement at 2-Hz stimulation of limb-girdle muscles, but no defect in neuromuscular transmission was present in her intercostal muscles.

The two sisters harbored a homozygous p.Glu1233Lys (9c.3698A>C) mutation in *LRP4*. Both had moderately severe fatigable weakness of the truncal and limb-girdle muscles with mild limitation of the ocular ductions. An intercostal muscle biopsy of the older sister revealed abnormally small EPs (Fig. 2A and 2B) with reduced expression of AChR and AChE. Electron microscopy showed that most EPs had poorly differentiated or degenerate junctional folds (Fig. 2C). The amplitudes of the endplate potential (EPP), the miniature EPP (MEPP), and the quantal content of the EPP (*m*) were all markedly diminished. Expression studies revealed the mutant protein hinders LRP4 from binding, activating, and phosphorylating MuSK.[2] Treatment with albuterol sulfate improved the patients' symptoms.

PREPL deficiency–related myasthenia[5]

This CMS was investigated in collaboration with Luc Regal, Chantal Verhille, Sandra Meulemans, and John W.M. Creemers in Belgium.[5] The myasthenia was first identified in the context of two contiguous recessive deletions involving *SLC3A1,* which codes for the heavy subunit of the cystine dibasic and neutral amino acid transporter, and *PREPL*, a prolyl endopeptidase-like gene. PREPL is ubiquitously expressed, with the highest levels in brain, kidney, and muscle, in decreasing order.[6] Because mutations in *SLC3A1* in some patients cause isolated cystinuria, it was suspected that the myasthenia was caused by PREPL deficiency.[7,8] Indeed, the CMS patient harbored two mutations exclusively in *PREPL*: a large maternally inherited deletion and a paternally inherited stop codon mutation (p.Met270X).

The proband was hypotonic since birth, with eyelid ptosis and muscle weakness that were improved by pyridostigmine. She became stronger after 6 months of age, was weaned off pyridostigmine by 12 months, and learned to use a walker by 17 months.

Investigations at 6 months of age showed no EMG decrement on 2-Hz stimulation, a finding also noted in myasthenic infants whose small muscle fibers have an increased input resistance.[9] An anconeus muscle biopsy revealed an absence of PREPL in patient muscle fibers (Fig. 3) and EPs. Electron microscopy of 35 patient EPs revealed only minimal nonspecific alterations, but the MEPP and miniature EP current (MEPC) amplitudes were

reduced to ~ 40% of normal, and the quantal content of the EPP (*m*) was approximately one-half of that of a 16-month-old control subject. The reduced *m* was due to reduction of number of quanta available for release (*n*), whereas the probability of quantal release (*p*) was normal. The number of [^{125}I]α-bungarotoxin binding sites per EP was higher than in a 2-year-old normal control.

A reduced postsynaptic response to ACh, indicated by the decreased amplitude of the MEPP and MEPC despite robust AChR expression and normal AChR kinetics, pointed to reduced ACh content of the synaptic vesicles. This could stem from a defect in presynaptic choline transport,[10] choline acetyltransferase,[11] the vesicular ACh transporter,[12] or the vesicular proton pump.[13] Because the phenotype with reduced presynaptic choline transport is different,[10] another mechanism was assumed to be pathogenic. A known function of PREPL is to act as an effector of the clathrin-associated adaptor protein 1 (AP-1) by binding to its μ1A subunit to release AP-1 from target membranes. As the trafficking of the vesicular ACh transporter between the synaptic vesicle membrane and the cytosol depends on AP-1,[14] absence of PREPL provides a plausible explanation for reduced filling of synaptic vesicles with ACh. The reason for the decreased quantal content of the EPP could not be determined.

Presynaptic exocytosis–related myasthenias[15]

Exocytosis of the synaptic vesicles at central and neuromuscular synapses depends on concerted action of multiple proteins (Fig. 4). According to current knowledge, these include the soluble *N*-ethylmaleimide-sensitive factor attachment protein receptor (SNARE) complex that comprises the synaptic vesicle-associated synaptobrevin (v-SNARE) and presynaptic membrane–associated Snap25B[15] and syntaxin.[16] In the past 3 years, we identified pathologic mutations in the genes encoding Snap25B, Munc13-1, and synaptobrevin. Because synaptic proteins subserving exocytosis are also present in the brain, some affected patients also show abnormal cortical electrical activity and impaired cognitive development.

SNAP25B myasthenia[15]

A patient harboring a dominant *de novo* p.Ile67Leu (c.200T>A) mutation in *SNAP25B* was observed at 11 years of age (Fig. 5A). At birth, she was stiff and cyanotic and had multiple joint contractures. Later, she presented fluctuating muscle weakness, intermittent eyelid ptosis, and episodes of unresponsiveness without convulsions. Electroencephalography (EEG) revealed generalized atypical polyspike and wave discharges with diffuse slowing of the background rhythm. Her motor development was delayed. She walked a few steps at age 7 and after that used a walker. At age 11, she spoke few words, and her speech was echolalic, spastic, and ataxic. The brain magnetic resonance imaging (MRI) was normal.

Conventional histochemical studies of intercostal and serratus anterior muscles were normal. The cholinesterase reactive synaptic contacts on intercostal muscle fibers were pretzel shaped or ovoid and expressed AChR and AChE normally. Electron micrographs of 22 EPs revealed no structural abnormality (Fig. 5B). Intercostal muscle EP electrophysiology studies showed a slightly reduced MEPP amplitude, but the number of AChRs per EP was

normal. The quantal content of the EP potential (*m*) (Fig. 5C) and the number of readily releasable quanta (*n*) (Fig. 5D) were abnormally distributed, with some values significantly lower and some normal or higher than normal, suggesting somatic mosaicism that can occur when a mutation arises in a postzygotic cell.[17] The probability of quantal release (*p*) was reduced to 63% of normal.

Whole-exome sequencing revealed a *de novo* variant (p.Ile67Asn (c.200T>A)) in the highly conserved exon 5 of SNAP25B. Sanger sequencing confirmed the mutation in the patient and its absence in her parents. Therapy with 3,4-diaminopyridine, along with levetiracetam to prevent seizures, improved the patient's strength but not her ataxia.

We attribute the pathogenicity of the Ile67Asn mutation to replacement of a hydrophobic isoleucine by a hydrophilic asparagine in the SNARE complex, which likely disrupts or disfigures the coiled-coil configuration of the complex wherein α-helices are held together by strong hydrophobic interactions.[21] We confirmed this by two sets of experiments. First, we mixed liposomes, incorporating synaptobrevin with liposomes containing wild-type or mutant SNAP25B plus syntaxin in the presence or absence of 10 mM Ca^{2+} and monitored the resulting changes in particle size distribution with a dynamic light-scattering particle size analyzer. In the absence of Ca^{2+}, mixing the two sets liposomes caused no change in particle size distribution. In the presence of Ca^{2+}, particle size distribution shifted to the right upon mixing liposomes containing synaptobrevin with liposomes containing wild-type SNAP25B plus syntaxin ($P < 0.05$) (Fig. 6A), but mixing liposomes containing synaptobrevin and mutant SNAP25B plus syntaxin had no effect on the particle size distribution (Fig. 6B).

Because the SNARE proteins are expressed in both chromaffin cells and neurons, we monitored the depolarization-induced exocytosis of dense core vesicles from chromaffin cells transfected with DNA from wild-type, mutant, and mutant plus wild-type SNAP25B by amperometry.[17] In this system, exocytosis of each vesicle is signaled by a single temporally resolved spike.[18–20] This test revealed that depolarized mutant SNAP25B–transfected cells generated fewer and lower amplitude spikes than wild-type SNAP25B–transfected cells (Fig. 6C), and at the end of 1 min, the cumulative exocytotic events by the mutant transfected cells was only about 20% of that by the wild-type transfected cells (Fig. 6D). Moreover, cells cotransfected with both wild-type and mutant SNAP25B exocytosed vesicles at the same reduced rate as cells transfected with only the mutant SNAP25B, indicating that the I67N mutation has a dominant-negative effect.

MUNC13-1 myasthenia [21]

Outside the SNARE complex, Munc 18-1 stabilizes a folded closed conformation of syntaxin 1B.[22,23] Upon Ca^{2+} entry into the nerve terminal, Munc13-1 shifts the position of Munc-18 on syntaxin 1B and stabilizes the open conformation of syntaxin 1B (see schematic diagram in Fig. 4). Open syntaxin 1B, together with Munc 18-1 and Munc13-1, irreversibly associates with SNAP25B and synaptobrevin to form primed SNARE complexes, rendering the cognate synaptic vesicles ready for exocytosis.[24,25]

A Native American girl presented with severe myasthenic symptoms at birth. At 4 months of age, she could barely move and was microcephalic with her head circumference below the fifth percentile (Fig. 7). She had variable eyelid ptosis, a high-arched palate, a small jaw, thoracic kyphoscoliosis, clinodactily of the fifth digits, and flexion contractures of the proximal joints and knees. She had an intermittent squint but no other eye movements. The EEG showed 2–4 Hz background activity over the posterior head regions, nearly continuous multifocal sharp waves in the central regions, and periodic trains of sharp waves in both hemispheres without overt seizure activity. There was no electric response to photic or auditory stimulation.

EMG studies revealed abnormally low-amplitude CMAPs at rest and a 20–40% decrement of the fourth compared to the first evoked CMAP in different muscles. Brief 50-Hz stimulation of the ulnar nerve increased the CMAP amplitude from 0.8 mV to 4 mV, pointing to a presynaptic defect, as observed in Lambert-Eaton myasthenic syndrome (LEMS). Therapy with pyridostigmine and 3,4-diaminopyridine improved the patient's cough and cry but increased her limb strength only slightly. She became ventilator dependent after 10 months of age and had bacterial pneumonia associated with a prolonged respiratory arrest. She remained paralyzed and mute and died of respiratory failure at 50 months.

In vitro analysis of neuromuscular transmission in the anconeus muscle showed a marked defect in exocytosis: the MEPP frequency was only 2% of normal and depolarization of the nerve terminals was not improved by increasing the external K^+ concentration. The MEPP amplitude fell within the normal range, but the quantal content of EPP potential (m) was only 6% and the number of readily releasable quanta (n) only 10% of the corresponding control values, but the probability of quantal release (p) was normal. The number of α-bungarotoxin–binding sites per EP was normal for the patient's age.

Conventional histochemical studies of the anconeus muscle revealed marked type 2 fiber atrophy and type 1 fiber hypertrophy. AChR and AChE were strongly expressed at the patient EPs. Electron microscopy of the EPs showed no abnormality.

Whole-exome sequencing confirmed by Sanger sequencing revealed a homozygous nonsense mutation in the N-terminal domain of *MUNC13-1* (*UNC13A*), (NM_001080421.2; c.304C>T/p.Gln102*) Both parents were heterozygous for the same mutation. The mutant protein retains only 101 of the 1703 residues of Munc13-1 and, because it lacks the syntaxin binding site of Munc13-1, it relegates syntaxin 1B to a permanently inactive state akin to a knockout.

Inactivation of syntaxin 1B likely accounts for the patient's cortical hyperexcitability, because gene mutations of syntaxin 1B are associated with febrile seizures with or without epilepsy,[26] and haploinsufficiency of *STX1B* is associated with myoclonic astatic epilepsy.[27]

A recent publication provides an explanation for our patient's microcephaly by showing that syntaxin 1B has an obligatory role in maintenance of developing or mature neurons and illustrates impaired brain development in syntaxin 1A/1B double gene knockout mice.[28] We therefore attribute our patient's microcephaly to the truncating homozygous Munc13-1 gene

mutation that consigns syntaxin 1B to a permanently closed nonfunctional state akin to a knockout.

Synaptobrevin-1 myasthenia [29]

Synaptobrevin-1 CMS was investigated in collaboration with Rosana Scola and her coworkers.[29] A Brazilian girl born to first-cousin unaffected parents had severe myasthenic symptoms since birth, but her eye movements were only mildly restricted. At 6 months of age, she lacked head control and could not sit without support. She remained severely hypotonic and areflexic into her teens and died of respiratory failure at age at 14 years of age. EMG studies at 2 years of age revealed low-amplitude CMAPs on stimulation of multiple motor nerves that decremented upon 3-Hz stimulation. Stimulation of the same nerves with 100 stimuli at 20 Hz increased the CMAP amplitude 2.3- to 8.8-fold, resembling the EMG findings in Lambert-Eaton syndrome. The brain MRI was normal. Biopsy specimens of the biceps brachii and quadriceps muscles only showed type 2 fiber atrophy.

Whole-exome sequencing of patient DNA revealed a homozygous N-terminal frameshifting single-nucleotide deletion (p.Ile114SerfsTer72 (c.340delA)) in *SYB1* in the patient and a single heterozygous mutation in each parent. *SYB1* has four alternatively spliced isoforms (A–D) with 3–5 C-terminal amino acids located within the synaptic vesicles. We identified mRNA for isoforms 1A and 1D in normal spinal cord anterior gray columns and skeletal muscle and assumed that either or both isoforms are expressed at motor nerve terminals. The mutation in each isoform is located at the 3′-end of the SYB1 transmembrane domain. It elongates the intravesicular C-terminus of SYB1A from 5 to 71 residues and of SYB1D from 4 to 31 residues. The elongated intravesicular residues hinder exocytosis by increasing the energy required to move the C-terminus of either isoform into the synaptic vesicle membrane, which is a key step in vesicle exocytosis.

Expression of wild-type and mutant isoforms in HEK cells revealed that expression of the mutant A and D isoforms was reduced to 15% and 68%, respectively, of the corresponding wild-type isoform. Finally, an amperometric assay of depolarization-evoked exocytosis of dense-core vesicles from chromaffin cells after forced expression with wild-type and mutant SYB1 A and D isoforms revealed that cells transfected with the mutant A and D isoform generated smaller spikes and exocytosed dense-core vesicles at a much slower rate than wild type, reducing the released catecholamine molecules to 2% and 12% of that released by wild-type transfected cells, respectively.

Conclusions

The CMS are caused by a diversity of targets and molecular mechanisms. Increased understanding of these syndromes has come from structural, electrophysiologic, and cytochemical investigations of the neuromuscular junctions of affected patients and from analyzing the effects of the mutant proteins engineered into heterologous cells. Monitoring the rate of synaptic vesicle exocytosis from depolarized bovine chromaffin cells transfected with wild-type and mutant Snap25B or synaptobrevin-1 proved to be a powerful tool for

estimating the effects of the mutant proteins on synaptic vesicle exocytosis. Finally, we predict that additional congenital myasthenic syndromes exist and await their discovery.

Acknowledgments

This work was supported by NIH Grant NS6277 to A.G.E.

References

1. Ohkawara B, Cabrera-Serrano M, Nakat T, et al. LRP4 third β-propeller domain mutations cause novel congenital myasthenic syndrome by compromising agrin-mediated MuSK signalling in a position-specific manner. Hum Mol Genet. 2014; 23:1856–1868. [PubMed: 24234652]
2. Selcen D, Ohkawara B, Shen X-M, McEvoy K, Ohno K, Engel AG. Impaired development and maintenance of the neuromuscular junction in LRP4 myasthenia. JAMA Neurology. 2015; 72:889–896. [PubMed: 26052878]
3. Burden SJ, Yumoto N, Zhang W. The role of MuSK in synapse formation and neuromuscular disease. Cold Spring Harb Perspect Biol. 2013; 5:a009167–a009167. [PubMed: 23637281]
4. Selcen D, Ohkawara B, Shen XM, et al. Impaired Synaptic Development, Maintenance, and Neuromuscular Transmission in LRP4-Related Myasthenia. JAMA Neurol. 2015; 72:889–896. [PubMed: 26052878]
5. Regal L, Shen XM, Selcen D, et al. PREPL deficiency with or without cystinuria causes a novel myasthenic syndrome. Neurology. 2014; 82:1254–1260. [PubMed: 24610330]
6. Martens K, Derua R, Meulmans S, et al. PREPL: a putative novel oligopeptidase propelled into the limelight. Biol Chem. 2006; 387:879–883. [PubMed: 16913837]
7. Jaeken J, Martens K, Francois I, et al. Deletion of PREPL, a gene encoding a putative serine oligopeptidase, in patients with hypotonia-cystinuria syndrome. American Journal of Human Genetics. 2006; 78:38–51. [PubMed: 16385448]
8. Boonen K, Regal L, Jaeken J, et al. PREPL: a putative novel oligopeptidase-like enzyme by name only? Lessons from patients. CNS Neurolog Disord Targets. 2011; 10:355–360.
9. Engel AG, Nagel A, Walls TJ, et al. Congenital myasthenic syndromes. I. Deficiency and short open-time of the acetylcholine receptor. Muscle Nerve. 1993; 16:1284–1292. [PubMed: 8232383]
10. Barwick KES, Wright J, Al-Turki S, et al. Defective presynaptic choline transport undelies hereditary presynaptic motor neuropathy. American Journal of Human Genetics. 2012; 91:1103–1107. [PubMed: 23141292]
11. Ohno K, Tsujino A, Shen XM, et al. Choline acetyltransferase mutations cause myasthenic syndrome associated with episodic apnea in humans. Proc Natl Acad Sci USA. 2001; 98:2017–2022. [PubMed: 11172068]
12. Prado VF, Martins-Silva C, de Castro BM, et al. Mice deficient for the vesicular acetylcholine transporter are myasthenic and have deficits in object and social recognition. Neuron. 2006; 51:601–612. [PubMed: 16950158]
13. Usdin TB, Eiden LE, Bonner TI, et al. Molecular biology of the vescular ACh transporter. Trends in Neurosciences. 1995; 18:218–224. [PubMed: 7610492]
14. Kim MH, Hersh LB. The vesicular acetylcholine transporter interacts with clathrin-associated adaptor complexes AP-1 and AP-2. J Biol Chem. 2004; 279:12580–12587. [PubMed: 14724281]
15. Shen XM, Selcen D, Brengman J, et al. Mutant SNAP25B causes myasthenia, cortical hyperexcitability, ataxia, and intellectual disability. Neurology. 2014; 83:2247–2255. [PubMed: 25381298]
16. Sudhof TC. Neurotransmitter release: The last millisecond in the life of the synaptic vesicle. Neuron. 2013; 80:675–690. [PubMed: 24183019]
17. Strachan, T., Read, AR. Human Molecular Genetics. 4. New York: Garland Science; 2011. Genes in pedigrees and populations; p. 61-90.

18. Leszczyszyn DJ, Jankkowski JA, Viveros OH, et al. Nicotinic receptor-mediated catecholamine release from individual chromaffin cell. Journal of Biological Chemistry. 1990; 265:14736–14737. [PubMed: 2394692]
19. Wightman RM, Jankowski JA, Kennedy RT, et al. Temporarily resolved catecholamine spikes correspond to single vesicle release from individual chromaffin cells. Proc Natl Acad Sci USA. 1991; 88:10754–10758. [PubMed: 1961743]
20. Criado M, Gil A, Viniegra S, et al. A single amino acid near the C terminus of the synaptosome associated protein 25 kDA (SNAP-25) is essential for exocytosis from chromaffin cells. Proc Natl Acad Sci USA. 1999; 96:7256–7261. [PubMed: 10377401]
21. Engel AG, Selcen D, Shen XM, et al. Loss of MUNC13–1 function causes microcephaly, cortical hyperexcitability, and fatal myasthenia. Neurol Genet. 2016; 2:e105. [PubMed: 27648472]
22. Dulubova I, Sugita S, Hill S, et al. A conformational switch in syntaxin during exocytosis: role of munc18. EMBO J. 1999; 18:4372–4382. [PubMed: 10449403]
23. Misura KM, Scheller RH, Weis WI. Self-association of the H3 region of syntaxin 1A. Implications for intermediates in SNARE complex assembly. J Biol Chem. 2001; 276:13273–13282. [PubMed: 11118447]
24. Ma C, Su L, Seven AB, et al. Reconstitution of the vital functions of Munc18 and Munc13 in neurotransmitter release. Science. 2013; 339:421–425. [PubMed: 23258414]
25. Rizo J, Xu J. The Synaptic Vesicle Release Machinery. Annu Rev Biophys. 2015; 44:339–367. [PubMed: 26098518]
26. Schubert J, Siekierska A, Langlois M, et al. Mutations in STX1B, encoding a presynaptic protein, cause fever-associated epilepsy syndromes. Nat Genet. 2014; 46:1327–1332. [PubMed: 25362483]
27. Vlaskamp DR, Rump P, Callenbach PM, et al. Haploinsufficiency of the STX1B gene is associated with myoclonic astatic epilepsy. Eur J Paediatr Neurol. 2016; 20:489–492. [PubMed: 26818399]
28. Vardar G, Chang S, Arancillo M, et al. Distinct functions of syntaxin-1 in neuronal maintenance, synaptic vesicle docking, and fusion in mouse neurons. J Neurosci. 2016; 36:7911–7924. [PubMed: 27466336]
29. Shen CM, Scola RH, Lorenzoni PJ, Kay CS, Werneck LC, Brengman J, Selcen D, Engel AG. Novel synaptobrevin-1 muation causes fatal congenital myasthenic syndrome. Ann Clin Transl Neurol. 2017; 4:130–138. [PubMed: 28168212]
30. Engel, AG. Congenital myasthenic syndromes. Medlink Neurology. 2017. http://www.medlink.com/MedLinkContent.asp

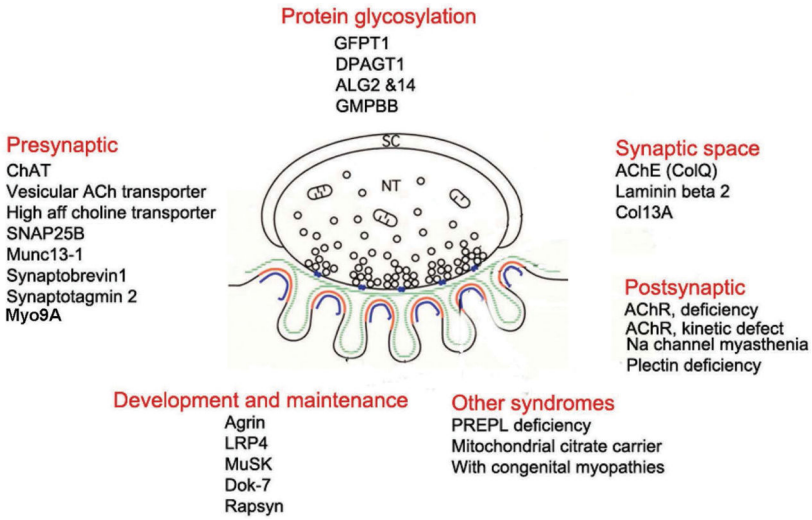

Figure 1.
Classification of the currently recognized congenital myasthenic syndromes.

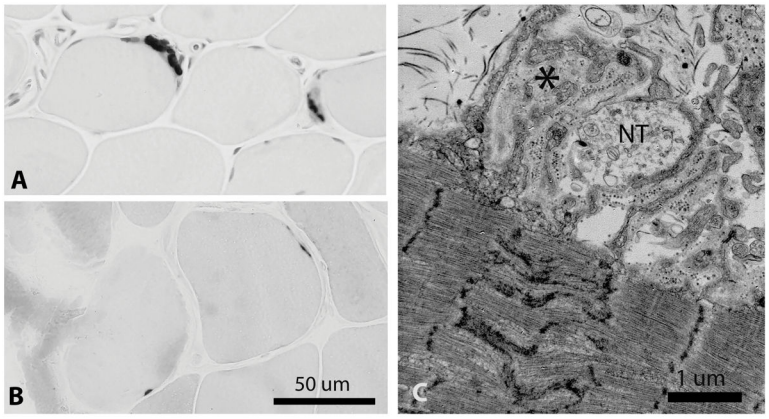

Figure 2.

Structural EP abnormalities in LRP4 myasthenia. In cholinesterase-stained transverse sections, the patient EPs (B) are much smaller than the control EPs (A). (C) Some EPs display poorly developed or degenerating junctional folds (asterisk), and some postsynaptic regions show focal myofibrillar degeneration. NT, nerve terminal; SC, Schwann cell.

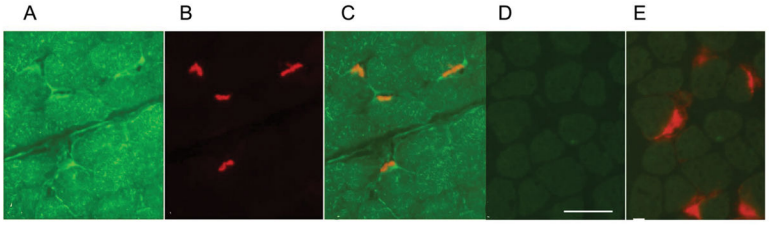

Figure 3.

PREPL and AChR localization in muscle fibers and EPs. (A) PREPL immunolocalization in control muscle fibers and EPs (green signal). (B) Serial section stained for AChR with rhodamine-labeled α-bungarotoxin shows presence of AChR at EPs (red signal). (C) Merged image of (A) and (B). (D) Patient muscle fibers and EPs fail to stain for PREPL. (E) Serial section to (E) stained for AChR shows presence of EPs. Color version shown online. Reproduced from Ref. 5 with permission of Kluwer and Bucy.

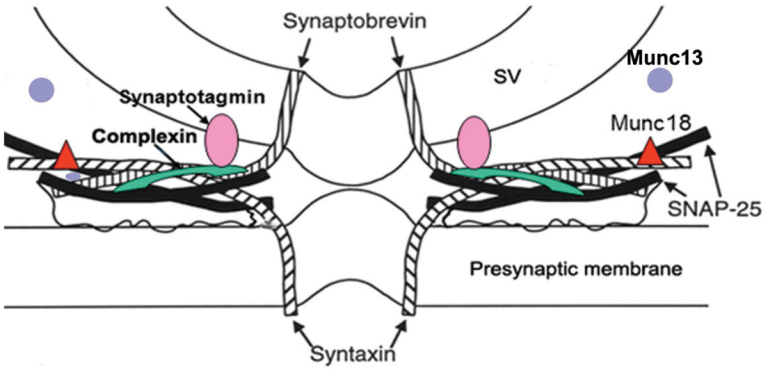

Figure 4.

Schematic diagram of the SNARE complex. Synaptobrevin anchored in the SV membrane (V-snare) and syntaxin-1 and SNAP25B (T-snares) anchored in the presynaptic membrane subserve vesicle exocytosis. Each SNARE protein is in a coiled-coil configuration. Complexin clamps the SNARE proteins at rest by binding to the groove between synaptobrevin and syntaxin. Ca^{2+} entry into the nerve terminal removes the inhibitory effect of complexin. Munc18-1 inhibits fast exocytosis by binding to a folded inactive form of syntaxin-1. Upon Ca^{2+} entry into the nerve terminal, Munc13 opens syntaxin-1 by displacing Munc18-1. This enables the SNARE complex to assemble, which primes the synaptic vesicles for release.

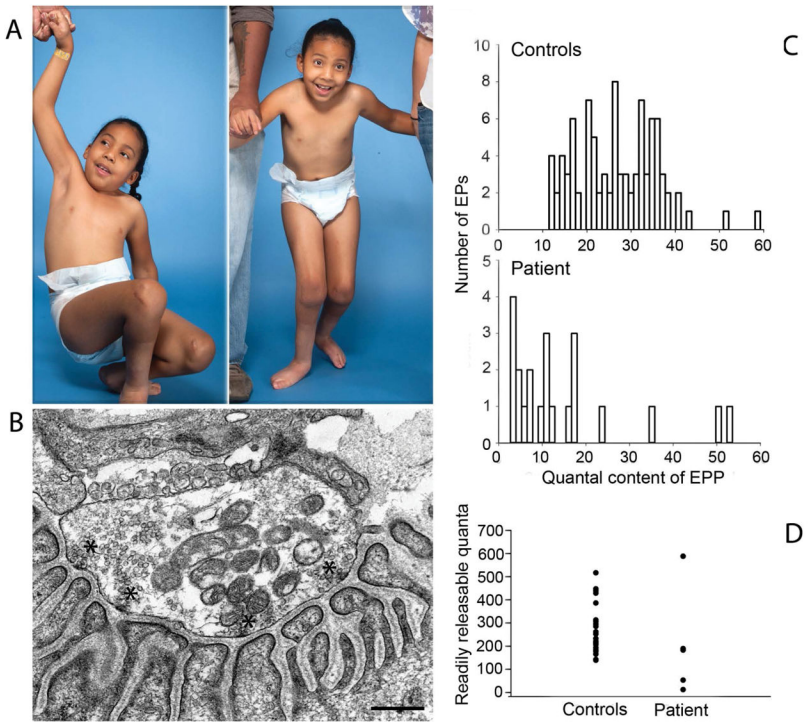

Figure 5.

SNAP25B CMS. (A) Patient at age 10 cannot rise from the floor or walk without assistance. (B) Electron micrograph of patient EP shows that the nerve terminal harbors abundant synaptic vesicles. Asterisks indicate vesicles focused on the active zones. The postsynaptic region is well developed. Bar = 0.5 μm. (C) Histograms of the quantal content of the EPP (*m*). The patient values are not normally distributed, with some values much lower and some normal or higher than normal. (D) Vertical scatter plot of readily releasable quanta (*n*) at patient and control EPs. Some values at patient EPs are much lower and some as high or higher than at control EPs. Reproduced from Ref. 15 with permission of Kluwer and Bucy.

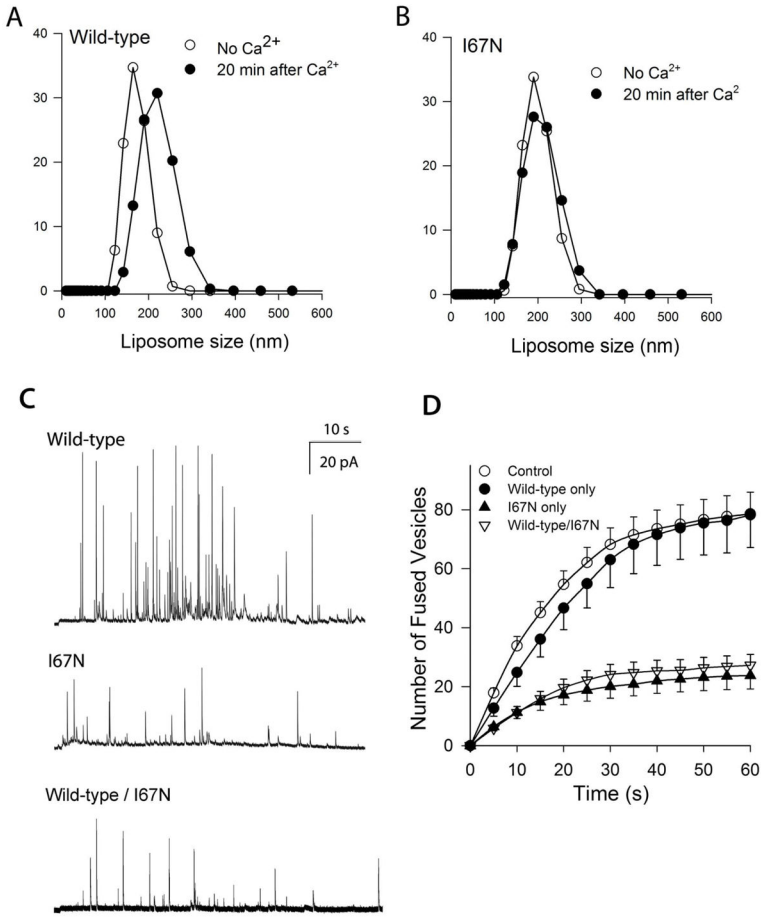

Figure 6.

Expression studies. (A) Mixing liposomes incorporating wild-type v- and t-SNARES causes a significant right shift in particle size distribution. (B) Mixing liposomes incorporating wild-type v-SNARE with t-SNARE liposomes harboring mutant Snap25B causes no significant shift in particle size distribution. (C) Representative amperometric traces from depolarized chromaffin cells. Each spike represents a single exocytotic event. Mutant SNAP25B- and mutant SNAP25B plus wild-type–transfected cells generate fewer and lower-amplitude spikes than wild-type SNAP25B–transfected cells. (D) Cumulative exocytotic events during the first minute after depolarization from 15 nontransfected, 11 wild-type SNAP25B–transfected, 14 mutant SNAP25B–transfected, and 17 mutant SNAP25B plus wild type–transfected cells. For each group of cells, each point indicates the mean number of spikes over 5 seconds. Vertical lines indicate one SE. Compared with nontransfected or wild type–transfected cells, mutant- transfected, or mutant plus wild-type–transfected cells, cells exocytose vesicles at similar markedly reduced rates. Reproduced from Ref. 15 with permission of Kluwer and Bucy.

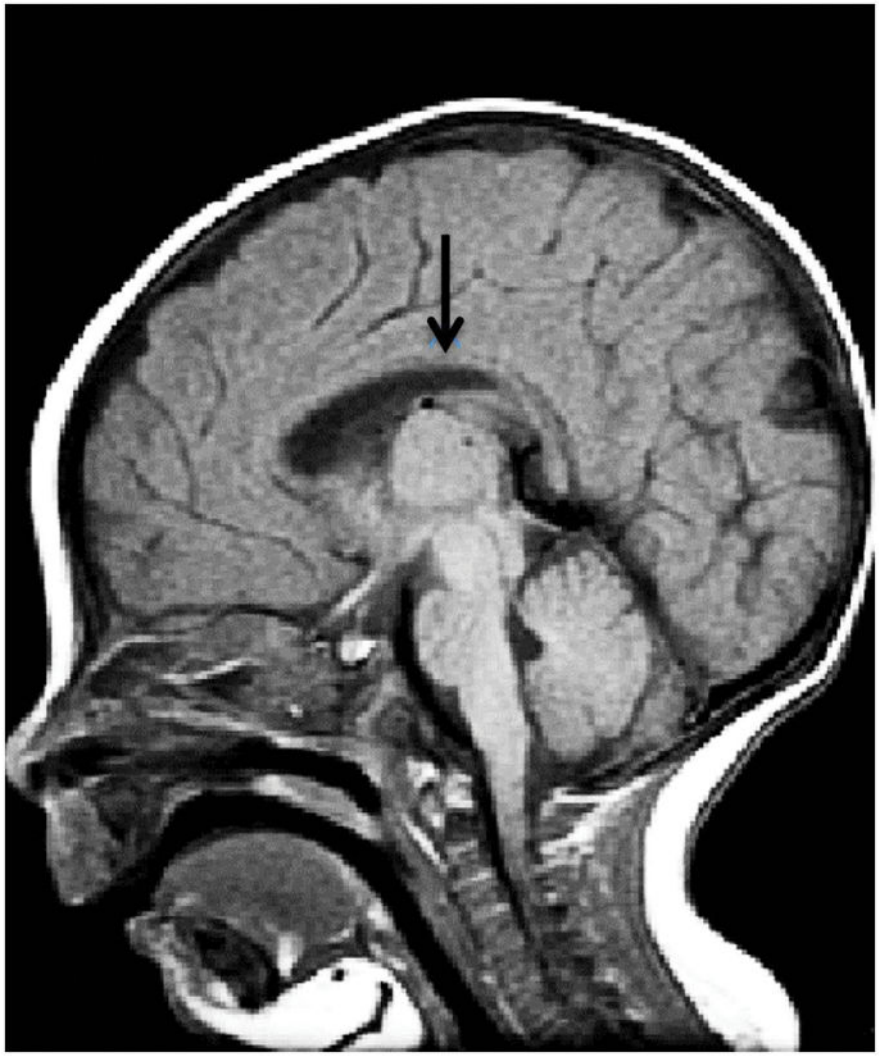

Figure 7.
Head MRI at age 4 months. The image shows small brain reflected by the size of the small corpus callosum (arrow). Reproduced from Ref. 15 with permission of Kluwer and Bucy.

Table 1

Classification of the CMS identified at the Mayo Clinic and other medical centers.[30]

	Index cases, Mayo Clinic	Proportion %
Presynaptic		
• Choline acetyltransferase deficiency[a]	18	5
• SNAP25B deficiency[a]	1	0.3
• Synaptotagmin 2 myasthenia[b]	0	0
• Paucity of synaptic vesicles and reduced quantal release	1	0.3
• Vesicular ACh transporter deficiency[b]	0	0
• High-affinity presynaptic choline transporter[b]	0	0
• Myosin 9a deficiency[b]	0	0
• Munc13-1 myasthenia	1	0.3
• Synaptobrevin-1 myasthenia	1	0.3
Synaptic space		
• Endplate AChE deficiency[a]	45	12.6
• Laminin β_2 deficiency[a]	1	0.3
• COL13A1 myasthenia[b]	0	0
Postsynaptic		
• Primary kinetic defect ± AChR deficiency[a]	63	17.6
• Primary AChR deficiency ± minor kinetic defect[a]	118	33
• Na channel myasthenia[a]	1	0.3
• Plectin deficiency[a]	2	0.6
Defects in endplate development and maintenance		
• Agrin deficiency[a]	3	0.9
• LRP4 deficiency[a]	2	0.6
• MuSK deficiency[a]	1	0.3
• Dok-7 myasthenia[a]	35	9.8
• Rapsyn deficiency[a]	51	14.2
Defects in protein glycosylation		
• GFPT1 myasthenia[a]	11	3.1
• DPAGT1 myasthenia[a]	2	0.6
• ALG2 myasthenia[b]	0	0
• ALG14 myasthenia[b]	0	0
• GMPPB myasthenia[b]	0	0
Other syndromes		
• PREPL deficiency myasthenia	1	0.3

	Index cases, Mayo Clinic	Proportion %
• Mitochondrial citrate carrier deficiency[b]	0	0
• Myasthenic syndrome with centronuclear myopathy	1	0.3
Total	358	

Note: Classification is based on cohort of CMS patients investigated at the Mayo Clinic between 1988 and 2017.

[a] Genetic defect detected.

[b] Identified at other medical centers.